Progress In Electromagnetics Research, Vol. 137, 389–406, 2013

A THEORETICAL MODEL FOR THE FREQUENCY-DEPENDENT DIELECTRIC PROPERTIES OF CORNEAL TISSUE AT MICROWAVE FREQUENCIES

Mehrdad Saviz[1, *] and Reza Faraji-Dana[2]

[1]Antenna Laboratory, School of Electrical and Computer Engineering, University of Tehran, P. O. Box 14395-515, North Kargar Avenue, Tehran, Iran

[2]Center of Excellence on Applied Electromagnetic Systems, School of Electrical & Computer Engineering, University of Tehran, P. O. Box 14395-515, North Kargar Avenue, Tehran, Iran

Abstract—This paper presents a structured model of the dielectric properties of the corneal tissue at microwave frequencies, based on the fine structure and chemical composition of its constituents. This is accomplished by appropriately combining the known properties of tissue substructures using mixing rules, in order to obtain the effective macroscopic properties of the medium. The presented approach is multi-scale: it begins from the microscopic scale and derives the macroscopic properties after several scale-steps. The predictions of the model agree with the existing measured data in the literature. Verification and analysis of the model sensitivity to input parameters have been presented. The model is expected to find application in non-invasive medical sensing where it can relate dielectric response to pathological structural changes in the tissue. The model is also useful for the prediction of dielectric properties for high-frequency computational dosimetry, and for understanding the physical mechanisms behind the macroscopic dielectric behaviour in general.

1. INTRODUCTION

Dielectric properties of biological tissues have been of interest for several reasons. They provide physical measures that are closely related to the underlying microstructure and chemical composition, can

Received 25 November 2012, Accepted 11 January 2013, Scheduled 26 February 2013

* Corresponding author: Mehrdad Saviz (msaviz@ut.ac.ir).

be used as indicators for non-invasive diagnosis and medical sensing [1–3], and are useful for computational dosimetry of electromagnetic waves [4–8] or computational evaluation of propagation in tissues for communication with biomedical devices [9, 10]. Data on dielectric properties can be obtained through spectroscopic measurements [11]. As recently shown [12, 13], dielectric properties of tissues can also be theoretically estimated and reproduced by considering the microstructure and material composition of the tissue, and quasi-electrostatic field solutions. Theoretical models are independent of direct spectroscopic measurements, and rely on appropriately combining the known properties of different, basic constituents (which is known as "Mixing"). Walker et al. [12] used a theoretical tissue model for cervical squamous tissue. A theoretical skin model has been developed in the MHz range by Huclova et al. [13] for non-invasive sensing, based on the effective medium approach, mixing formulas and numerical analysis. Theoretical models are extremely useful in non-invasive medical sensing, because they provide a connection between tissue structure and dielectric response. Pathological changes in tissue microstructure (e.g., cancer) cause changes in the dielectric response, which can be interpreted based on the theoretical model [14].

Recently, studies of radiation safety are in progress which involve computational evaluation of THz absorption in superficial tissues; i.e., the skin and the eyes (esp. the cornea) [15]. As is well-known, experimental data on dielectric properties of tissues are rather scarce in this frequency region. In such applications, a theoretical model might be the most promising option for estimating the dielectric properties of tissues and their substructures. Obviously, once such a model is developed, it should be verified using the existing experimental data at lower frequencies (e.g., microwaves).

Theoretical models of skin have been reported in the RF frequency range [13]. To the best of our knowledge, a theoretical electromagnetic model for the cornea has not yet been developed. Applications for this model can be anticipated in computational dosimetry and non-invasive sensing [14, 15].

We provide, for the first time, a theoretical electromagnetic model for predicting the electrical properties of the corneal tissue based on its physical microstructure and chemical composition. Interestingly as we shall see, the cornea is quite amenable to theoretical analysis for two reasons: Because of its role in vision, the cornea is a highly ordered tissue. This fact facilitates modeling by relatively simple mixture rules. Moreover, corneal hydration (water content) is actively and strictly controlled in the eye and is kept almost constant in a healthy tissue. We thus expect good comparison with experimental datasets to be

feasible within a reasonable uncertainty. These features are not present in the case of skin, where notable differences arise between wet and dry states.

Objective: Our purpose is to develop a theoretical cornea model with sufficient complexity to agree within ±20% or better with available measured values in the microwave region.

Perhaps the most extensively used set of experimental tissue data to date are those of Gabriel et al., compiled in [4] based on the works of Gabriel et al. [16, 17] up to 100 GHz. In the early 2000s, a group of researchers including C. Gabriel performed new dielectric measurements in vivo and in vitro as well as a literature review [18]. As concerns the cornea, the experimental results were close to the previous results of Gabriel et al. [17, 19].

In this paper, we use Cole-Cole and Debye expressions to express the complex frequency-dependent dielectric properties of basic constituents such as water. Many dielectric relaxation processes in basic materials can be meaningfully described by the Cole-Cole expression for the complex permittivity ε, as in Eq. (1):

$$\varepsilon = \varepsilon_\infty + \frac{\Delta\varepsilon}{1 + (j2\pi f\tau)^{1-\alpha}} + \frac{\sigma_i}{j\omega\varepsilon_0} \tag{1}$$

where $\Delta\varepsilon = (\varepsilon_s - \varepsilon_\infty)$. The expression in (1) reproduces one relaxation from a higher permittivity ε_s at lower frequencies to a lower permittivity ε_∞ at higher frequencies, with the transition taking place at the relaxation frequency $f = (2\pi\tau)^{-1}$. The parameter α varies between 0 and 1, with higher values expressing broader dispersions. The special case of $\alpha = 0$ corresponds to a Debye expression with an additional conductivity term. The symbol σ_i stands for ionic conductivity [17]. The ionic conductivity is more important at lower frequencies.

In the following, Section 2 introduces the relevant structural information about the cornea. Section 3 presents the procedure of theoretical modeling. Section 4 then follows with comparison with experimental data and discussion.

2. THE STRUCTURE AND COMPOSITION OF CORNEA

The cornea is a living tissue in the outer surface of the eyeball. In humans it has a thickness of almost 0.5 millimeter, and comprises five discernible layers. These are, from the outermost to the innermost, the epithelium; Bowman's membrane; the stroma; Descemet's membrane, and the endothelium [20]. These are graphically reproduced in

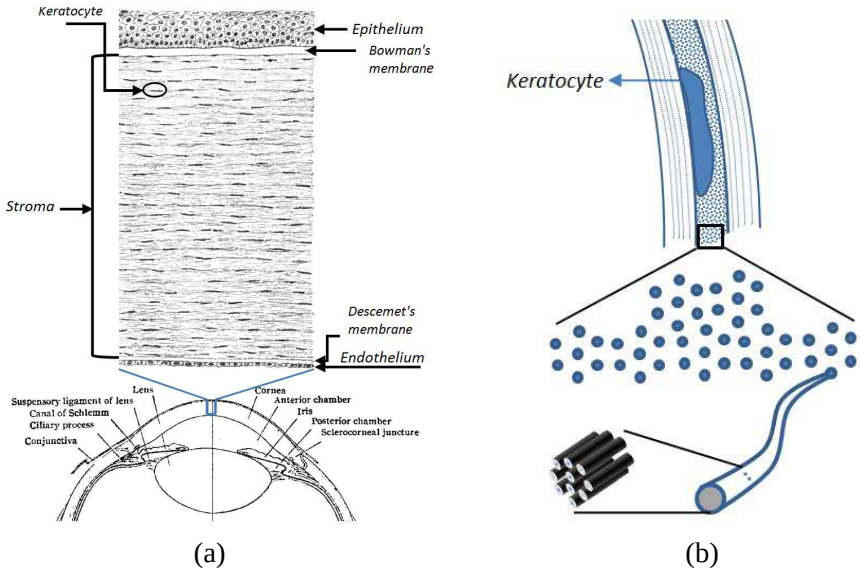

Figure 1. (a) The five layers of the human cornea from [46]. (b) Magnification of the marked region, showing three (out of about 200) lamellae and a keratocyte. Fibril orientations are shown here as either in or onto the page. Bottom: Each section of a collagen fibril itself is an arrangement of long collagen molecules.

Figure 1(a). The epithelium and endothelium layers consist of tightly packed cells (Table 1). In humans the epithelium consists of approximately 6 layers of cells, whereas the 5 μm thick endothelium layer consists of a single layer of cells only [20]. The Bowman's and Descemet's membranes are relatively thin, tough layers, rich in collagen fibrils [21] and both about 10–20 μm thick. Collagen is the name of a family of organic molecules that can provide for high tensile strength by forming very long fibrils [22]. The stroma can be described as being composed of collagen fibrils in an aqueous background (the ground substance). A sparse distribution (a volume fraction of about 12%) of cells (keratocytes, Figure 1(b)), rest between the lamellae [23]. The ground substance of the stroma is itself composed of water and other non-fibrilar components [20]. The stroma is of dominant importance in our treatment here, since it constitutes 90% of the whole cornea [20].

A closer study of the stroma reveals that long collagen fibrils run across the stroma as shown in Figure 1(b) [24]. One can consider the stroma as composed of stacked lamellae, where the orientations of the fibrils in each lamella are identical, but at specific angles with respect

Table 1. Model parameters.

Symbol	Description	Value (Human)	Value (Porcine)	References
d_{epi}	Thickness of the epithelium	50 µm	80 µm	[20, 38]
d_{endo}	Thickness of the endothelium	5 µm	8 µm	[38, 39]
d_s	Thickness of the stroma	500 µm	800 µm	[39] and [20, 38]
d_{cornea}	Corneal thickness	$\sim$ 555 µm	$\sim$ 888 µm	[20, 38]
v_c	Collagen volume fraction in stroma	0.124	0.124	[40]
v_{nf}	Volume fraction of non-fibrilar material from ground substance	0.104	0.104	[40]
-	Diameter of a collagen fibril	30.8 nm	36.9 ± 3.2 nm	[26]
-	Interfibrilar distance	55.3 ± 4.00 nm	58.6 ± 4.5 nm	[26]
ε_c	Permittivity estimation for collagen	2.4	2.4	[41]
ε_{nf}	Permittivity approximation for non-fibrilar material in the stromal ground substance (ions, macromolecules)	3 (2–5)	3 (2–5)	[30, 31]
v_{kerato}	Mean volume fraction of keratocytes in the stroma	0.122	0.111	[23, 42]

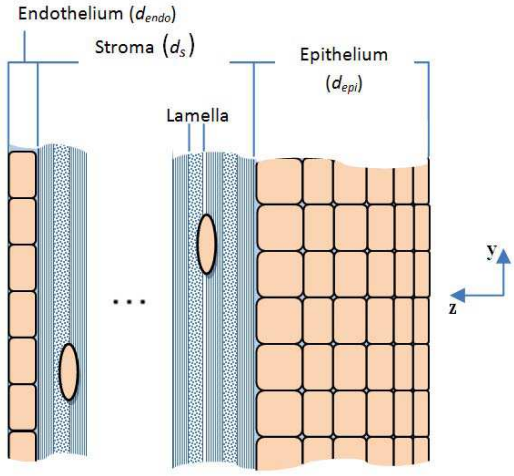

Figure 2. The idealized model of the cornea.

to adjacent lamellae. Specifically, fibrilar orientations from adjacent lamellae tend to be at right angles to each other in the central region of the cornea [25], as shown in Figure 1(b). The lamellae might branch and interweave at some points. Interweaving of the lamellae has been ignored in the model.

In terms of composition, Table 1 shows the dimensions of the fibrils, volume fractions, and other geometrical parameters we shall use in this study. In Table 1, we observe the similarity of collagen volume fractions for human and porcine tissues. As Meek and Leonard [26] show in their experimental study of cornea ultrastructure in 45 types of species, the fibrilar volume fraction, and intra-fibrilar spacing between collagen molecules is almost constant among mammals; a fact which is further justified by considering the small variation of the optical refractive index of the cornea among species; namely $n_{cor} = 1.372 \pm 0.009$ [26].

3. THE CORNEA MODEL

3.1. Preliminary Considerations

The idealized model we shall use for the cornea is depicted in Figure 2. The Bowman's and Descemet's membranes have been merged into the model for the stroma. This is justified by the similar collagen-based composition of these layers when compared to the stroma.

Furthermore, it has been shown experimentally in [27] that samples of stroma with or without the Descemet's membrane have almost the same permeability to ions and several larger molecules, indicating that the Descemet's membrane is actually not an electrically "impeding" membrane, as is observed, e.g., with cell membranes.

We note that the structure is anisotropic. With reference to the coordinates in Figure 2, it is desired to calculate the effective dielectric tensor $\bar{\varepsilon}_{cor}$

$$\bar{\varepsilon}_{cor} = \begin{pmatrix} \varepsilon_{cor}^{xx} & \varepsilon_{cor}^{xy} & \varepsilon_{cor}^{xz} \\ \varepsilon_{cor}^{yx} & \varepsilon_{cor}^{yy} & \varepsilon_{cor}^{yz} \\ \varepsilon_{cor}^{zx} & \varepsilon_{cor}^{zy} & \varepsilon_{cor}^{zz} \end{pmatrix} = \begin{pmatrix} \varepsilon_{cor}^{\|_\ell} & 0 & 0 \\ 0 & \varepsilon_{cor}^{\|_\ell} & 0 \\ 0 & 0 & \varepsilon_{cor}^{\perp_\ell} \end{pmatrix}, \tag{2}$$

where in order to facilitate the presentation, we introduce the following notational convention for field polarizations and their corresponding permittivities: superscripts $\|_\ell$ and $\perp_\ell$ indicate directions parallel or perpendicular to the planar lamellae (or to the surface of the cornea), respectively, and superscripts $\|_f$ and $\perp_f$ indicate direction parallel or perpendicular to linear collagen fibrils, respectively. Subscripts describe the medium to which the effective permittivity is assigned, and are defined where they first appear throughout the paper.

Practically, the process of computing the overall dielectric properties of the tissue (mixing) corresponds to replacing the heterogeneous material with a "homogenized" model, which has the same overall dielectric behaviour. There are numerous "mixture" rules that are derived for different geometries from rigorous field solutions. Mixture rules differ from simple spatial averaging of permittivity, unless for some special cases. A review of many useful mixture rules, including those used in this paper, can be found in [28]. We use the mixture rules with complex, frequency-dependent dielectric parameters as in [28]. In this way, we also incorporate material dispersions into the model.

Considering the cornea, one can distinguish several "scales" of electrical heterogeneity. The tissue is heterogeneous in the molecular, cellular, and also in the macroscopic tissue scales. The theoretical modeling of dielectric properties for the tissue begins by starting from the smallest scale, applying mixture rules, replacing the heterogeneity in that scale with a homogeneous model, and proceeding to the next, larger scale, where one has the homogenized model of the previous step among other constituents of the larger scale. The process of using mixture rules can now be repeated as in the previous step. The mixing steps are schematically shown in Figure 3 for the cornea.

At each scale, the process of mixing and the effective properties obtained are valid as long as the inclusions remain small with respect to

the wavelength. We consider electrically small to mean smaller than $\lambda_w/10$ or $\lambda_w/5$, with λ_w denoting the wavelength inside an aqueous background (Table 2). As a result, the cornea model with a stroma of 500 µm thickness is physically meaningful up to about 20 GHz. The consecutive steps in Figure 3 are now briefly described.

3.2. The Model

3.2.1. The Aqueous Ground Substance

To estimate the complex permittivity of the ground substance in the stroma, first the ionic content in the ground substance is modeled by the addition of a conductivity term to the water model. The water model $\varepsilon_w(f)$ is given in Table 2. This yields the aqueous electrolyte

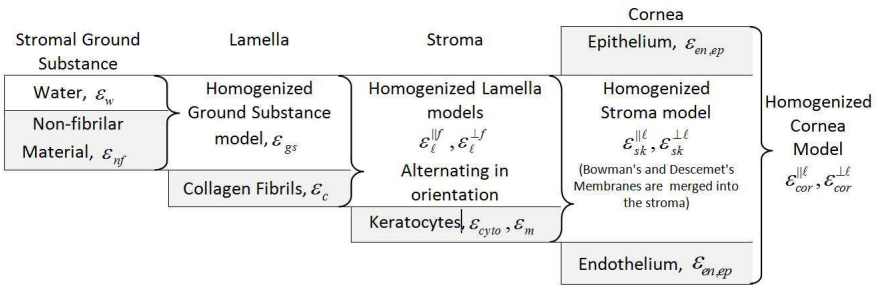

Figure 3. The hierarchy of scales: Mixing steps are shown schematically from the smallest to the macroscopic tissue scales.

Table 2. The double-Debye dielectric model of water [43].

Equation		
$\varepsilon_w = \varepsilon_\infty + \frac{(\varepsilon_1-\varepsilon_2)}{1+j2\pi f\tau_1} + \frac{(\varepsilon_2-\varepsilon_\infty)}{1+j2\pi f\tau_2}.$		
Symbol	Description	Value
ε_1	Static permittivity (37°C)	74.23
ε_∞	Limit permittivity at high frequencies	3.76
ε_2	Intermediate permittivity	4.98
τ_1	Time constant of the first relaxation	6.26 ps
τ_2	Time constant of the second relaxation	0.157 ps

permittivity ε_{lyt}:

$$\varepsilon_{lyt} = \varepsilon_w + \frac{\sigma_i}{j\omega\varepsilon_0} \tag{3}$$

The value of σ_i for most biological electrolytes is estimated to be on the order of $1\,\mathrm{S{\cdot}m^{-1}}$ (an example is discussed by Gimsa et al. [29]). We have used $\sigma_i = 1.35\,\mathrm{S{\cdot}m^{-1}}$. This value is close to $\sigma_i = 1.2\,\mathrm{S{\cdot}m^{-1}}$ mentioned by Huclova et al. [13] for biological electrolytes and provides slightly better comparison with experimental data.

Proteins and other macromolecules account for much of the non-fibrilar material volume fraction. The final permittivity of the ground substance is obtained by applying the Maxwell-Garnet (MG) Mixture rule, which assumes spherical particles of ε_{nf} in a background of ε_{lyt} [28] and by using the volume fraction of non-fibrilar material v_{nf} as given in Table 1.

$$\varepsilon_{gs} = \varepsilon_{lyt} + 3\,v_{nf}\varepsilon_{lyt}\frac{\varepsilon_{nf} - \varepsilon_{lyt}}{\varepsilon_{nf} + 2\varepsilon_{lyt} - v_{nf}\,(\varepsilon_{nf} - \varepsilon_{lyt})}. \tag{4}$$

We note that although the inclusions are of molecular dimensions, their effect can nevertheless be reasonably theoretically estimated by appropriate mixture rules according to the literature [30, 31]. Although it has been shown that the Bruggeman mixture formula can provide more accurate results than MG [32], our experience showed only minor difference between these formulas for the relatively low volume fractions here.

3.2.2. The Lamellae

Every lamella is composed of the aqueous ground substance and collagen fibrils as inclusions. We shall distinguish between two cases, i.e., where the electrical field vector is perpendicular to the fibrils, giving $\varepsilon_\ell^{\perp f}$, and where it parallels the fibrils, resulting in $\varepsilon_\ell^{\| f}$. We thus use the MG mixture formula for cylindrical inclusions [33] for $\varepsilon_\ell^{\perp f}$. The linear mixture law [28], which is the well-known formula for combination of parallel capacitors, is used to find $\varepsilon_\ell^{\| f}$

$$\varepsilon_\ell^{\perp f} = \varepsilon_{gs} + 2\,v_c\varepsilon_{gs}\frac{\varepsilon_c - \varepsilon_{gs}}{\varepsilon_c + \varepsilon_{gs} - v_c\,(\varepsilon_c - \varepsilon_{gs})}. \tag{5}$$

$$\varepsilon_\ell^{\| f} = \varepsilon_{gs}\cdot(1 - v_c) + \varepsilon_c \cdot v_c \tag{6}$$

3.2.3. The Stroma

With reference to Figure 2, the field component perpendicular to the lamellae $E^{\perp\ell} = E_z$ is always perpendicular to the fibrils, thus for $E^{\perp\ell}$

Table 3. Parameters for the cellular components (epithelium, endothelium, keratocytes).

Symbol	Description	Value	References
d_m	Thickness of the membrane	5.5 nm	[44]
d_{cyto}	Average cell diameter in the epi/endothelium	5 µm	[20]
d_{kerato}	Keratocyte body length	30.9 µm	[45]
t_{kerato}	Keratocyte thickness	1.34 µm	[45]
ε_m	Permittivity of lipid membrane models	9.0	[29]
ε_{cyt}	Complex permittivity of the cytoplasm	See text	[29]

all lamellae appear with the same permittivity $\varepsilon_\ell^{\perp f}$. We thus conclude that $\varepsilon_s^{\perp \ell} = \varepsilon_\ell^{\perp f}$. For $E^{\parallel \ell}$ (e.g., assuming either E_x or E_y in Figure 2) fibril orientations appear periodically parallel or perpendicular to the field, and we can use the linear mixture rule as in Eq. (6) to find the effective permittivity.

$$\varepsilon_s^{\parallel \ell} = \frac{1}{2}\left(\varepsilon_\ell^{\parallel f} + \varepsilon_\ell^{\perp f}\right). \tag{7}$$

$$\varepsilon_s^{\perp \ell} = \varepsilon_\ell^{\perp f} \tag{8}$$

To model the keratocytes dispersed throughout the stroma, the MG mixture rule for double layer spherical inclusions [28, Eq. (3.32)] is used with the volume fraction v_k and membrane (ε_m) and cytoplasm (ε_{cyto}) properties as described in Table 3. The cytoplasm is modeled based on the frequency-dependent cytoplasm parameters from Gimsa et al. [29]. specifically using the expression from Table 2 with $\varepsilon_1 = 212$, $\varepsilon_2 = 50$, $\varepsilon_\infty = 4$, $\tau_1 = 10.61\,\text{ns}$, $\tau_2 = 7.2\,\text{ps}$ and $\sigma_i = 1\,\text{S}\cdot\text{m}^{-1}$ with a Cole-Cole broadening factor of $\alpha_1 = 0.5$ (Eq. (1)). Letting ε_{sk} denote the complex permittivity of the stroma with keratocytes,

$$\frac{\varepsilon_{sk} - \varepsilon_s}{\varepsilon_{sk} + \varepsilon_s} = v_k \frac{(\varepsilon_m - \varepsilon_s)(\varepsilon_{cyt} + 2\varepsilon_m) + w(\varepsilon_{cyt} - \varepsilon_m)(\varepsilon_s + 2\varepsilon_m)}{(\varepsilon_m + 2\varepsilon_s)(\varepsilon_{cyt} + 2\varepsilon_m) + 2w(\varepsilon_{cyt} - \varepsilon_m)(\varepsilon_m - \varepsilon_s)}. \tag{9}$$

where $w = [(R - d_m)/R]^3$ with R denoting the cell radius and d_m the membrane thickness from Table 3. The value for R has been chosen equal to half the keratocyte thickness (Table 3). In Eq. (9), $\varepsilon_{sk}^{\perp \ell}$ and $\varepsilon_{sk}^{\parallel \ell}$ will be obtained, if ε_s is substituted by $\varepsilon_s^{\perp \ell}$ and $\varepsilon_s^{\parallel \ell}$, respectively.

3.2.4. The Cornea Model

Finally, for the last step in the model hierarchy, the stromal layer has to be considered as enclosed between the cellular epithelium and endothelium layers. These are modeled by cytoplasm (ε_{cyto}) and membranes (ε_m) of thickness d_m. For $\varepsilon_{cor}^{\perp\ell}$, the membranes parallel to the field can be neglected because of their extremely low volume fraction. The cell membranes perpendicular to the field orientation are considered because of their probable blocking effect against ionic currents (the well-known capacitive effect at poorly conducting membranes) at lower frequencies. These are then mixed by the well-known series capacitors formula; Eq. (10). The parameter $N_m = 14$ is the number of membrane layers, 12 due to 6 rows of epithelial cells and 2 due to one row of endothelial cells.

$$\varepsilon_{cor}^{\perp\ell} = (d_{en} + d_{ep} + d_s + N_m d_m) \cdot \left(\frac{d_{en} + d_{ep}}{\varepsilon_{cyto}} + \frac{N_m d_m}{\varepsilon_m} + \frac{d_s}{\varepsilon_{sk}^{\perp\ell}} \right)^{-1} \tag{10}$$

For $\varepsilon_{cor}^{\|\ell}$, we first take into account the horizontal membranes in Figure 2, by defining $\varepsilon_{en,ep}$ calculated by a series-capacitance rule Eq. (11), followed by a linear mixing rule in Eq. (12).

$$\varepsilon_{en,ep} = (d_{cyto} + 2d_m) \cdot \left(\frac{d_{cyto}}{\varepsilon_{cyt}} + \frac{2 \cdot d_m}{\varepsilon_m} \right)^{-1} \tag{11}$$

$$\varepsilon_{cor}^{\|\ell} = \frac{\varepsilon_{en,ep} \cdot (d_{en} + d_{ep}) + \varepsilon_{sk}^{\|\ell} \cdot d_s + N_m d_m \varepsilon_m}{d_{en} + d_{ep} + d_s + N_m d_m}. \tag{12}$$

The set of Formulas (3)–(12) constitutes a model for the cornea composed of smaller individual models.

4. RESULTS AND DISCUSSION

We compare the whole tissue permittivity and conductivity obtained from our model with experimental data models from the literature. The model parameters for porcine cornea from Table 1 are used to provide comparison with a recent set of cornea data [34] measured and reported for three age-groups of pigs over the 0.4–10 GHz frequency range. In accordance with the measurement procedures [35] which correspond to the parallel electric field polarization for the cornea, comparison is presented for $\varepsilon_{cor}^{\|\ell}$ in Figure 4 and in the rest of the paper. The model shows agreement with the experimental data within the usual experimental tolerance of 20%.

We now investigate a possible further refinement for the model. In Section 3, we used a free-water model in our analysis. A slight decrease

in relaxation frequency in the experimental data of Figure 4 from that predicted by the theoretical model (dashed line) suggests the presence of bound-water, which is usually slower than free water. We model the presence of bound water as in [36] by considering a certain volume fraction of water to have a principal relaxation time τ_h instead of τ_1 in Table 2. The model with bound water can have its relative difference reduced to within 5% (3% for one of the datasets) for the real part and

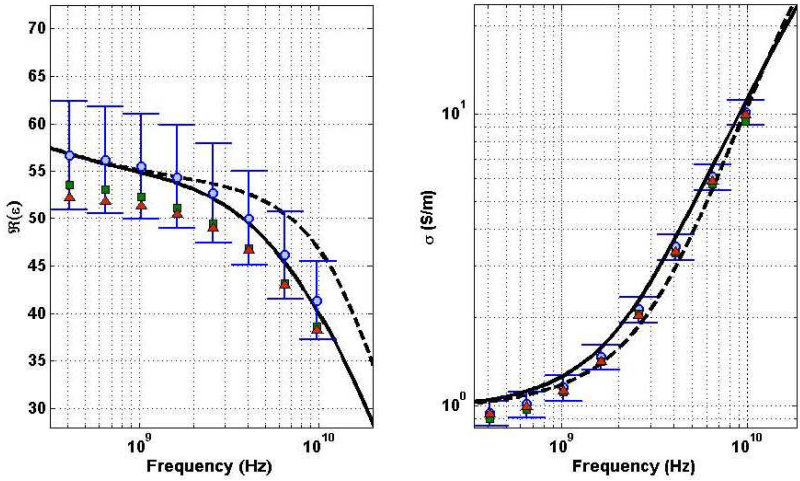

Figure 4. Model comparison; The conductivity is defined as $\sigma = \omega\varepsilon_0\Im(\varepsilon)$. Theoretical model with (solid lines) or without (dashed line) bound water model, compared to experimental data from [34] (Circles, squares and triangles refer to the three datasets of 10, 50 and 250 kg animals, respectively). Error-bars show indicate ±10% uncertainty.

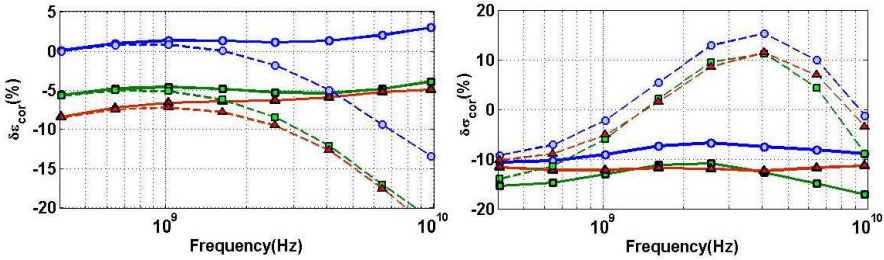

Figure 5. Relative difference of theoretical model with (solid lines) or without (dashed line) bound water, from experimental data [34]. Markers correspond to those of Figure 4.

to within nearly 17% (10% for one of the datasets) for the conductivity, well within the usual experimental uncertainty (Figures 4, 5). This model assumes a volume fraction of bound water equal to $v_b = 0.3$ and a relaxation time of $\tau_h = 4\tau_1$, which are reasonable values according to the literature [37].

Consequently as understood from Figure 5, inclusion of bound-water in the model is promising and seems to provide even better agreement especially at higher frequencies. However, it has not been included in the theoretical model of the previous section, mostly due to the uncertainties involved in related parameters. More detailed knowledge of bound water properties in the cornea can be used to refine the model in future.

Further comparison with experimental data is provided in the online supplement for both polarizations, and shows agreement within 20%. It is thus observed that the model reproduces the experimentally observed behaviour above several hundred MHz very well. The model has good accuracy also in the microwave region, which has been the target of this work.

In order to assess the meaningfulness of the model and the significance of its agreement with measured values, and to understand the model dependence on parameter values, we have also performed a sensitivity analysis for $\varepsilon_{cor}^{||\ell}(f)$. By defining the sensitivity S as the "ratio of relative changes", ε_{cor} (1 GHz) shows significant sensitivity to $v_c, (S = -0.14)$, and v_{nf}, $(S = -0.12)$, but shows insignificant dependence on ε_c and ε_{nf} $(S = 0.01)$ and σ_i $(S = 0.00)$. This can be understood by the relatively high dielectric permittivity of water at lower frequencies. Low-permittivity inclusions such as collagen occupy a certain volume, excluding a corresponding amount of water. This leads to a decrease in permittivity which is more sensitive to the excluded water volume, and less sensitive to the actual permittivity of the inclusions. Obviously, σ_{cor} (1 GHz) depends strongly on ionic content $(S = 0.65)$, but this dependence fades at higher frequencies, where the dielectric loss of water becomes dominant. Interestingly, as several high sensitivity values indicate, the good agreement is not trivial, but rather meaningfully related to the values chosen for the model parameters. A set of calculated sensitivity values for several model parameters is provided in the online supplement. The supplement also includes a description of further attempts at numerical verification of the cornea model.

One of the advantages of the theoretical model is its independence from measurements; it is not a mathematical expression fitted to experimental data, but rather a physics-based bottom-to-top method for theoretically reproducing a set of tissue properties over a wide

range of frequencies. Currently, refinement of the model using the aforementioned ideas, using the model for predicting the dielectric properties of corneal tissue sub-structures at higher frequencies for computational dosimetry, and some ophthalmological applications are under investigation.

5. CONCLUSION

We have presented a fine model for theoretical prediction of the complex permittivity of the cornea based on its material composition and by applying appropriate mixing rules to the microstructure of the cornea in several steps. Good agreement of the theoretical model predictions with reported experimental models in the literature have been obtained at microwave frequencies within the target accuracy of 20%. Sensitivity analysis for the model parameters have been performed, which provides support for the physical meaningfulness of the model. It has been shown that the model can be refined at higher frequencies by considering the effect of bound water. The model is expected to find application in non-invasive medical sensing and prediction of dielectric properties for high-frequency computational dosimetry.

ACKNOWLEDGMENT

M. Saviz expresses gratitude to Prof. Dr. M. Clemens, head of the Chair of Electromagnetic Theory at the University of Wuppertal for facilitating this research. Dr.-Ing. J. Streckert has kindly and carefully reviewed the manuscript and pointed out many improvements. Constructive discussions with Dr.-Ing. D. N. Chigrin are warmly appreciated. Prof. Dr.-Ing. V. Hansen has been supporting this work with helpful experience and encouragement. M. Sc. O. Spathmann has been helpful with the literature regarding experimental data. The work of M. Saviz is supported by a Grant from Iran Telecommunications Research Center.

REFERENCES

1. Huang, K., X. B. Xu, L. P. Yan, and M. Zhang, "A new noninvasive method for determining the conductivity of tissue embedded in multilayer biological structure," *Journal of Electromagnetic Waves and Applications*, Vol. 16, No. 6, 851–860, 2002.

2. Surowiec, A. J., S. S. Stuchly, J. R. Barr, and A. Swarup, "Dielectric properties of breast carcinoma and the surrounding tissues," *IEEE Transactions on Biomedical Engineering*, Vol. 35, 257–263, 1988.
3. Yan, L. P., K. M. Huang, and C. J. Liu, "A noninvasive method for determining dielectric properties of layered tissues on human back," *Journal of Electromagnetic Waves and Applications*, Vol. 21, No. 13, 1829–1843, 2007.
4. Gabriel, C., "Dielectric properties of body tissues in the frequency range 10 Hz–100 GHz," IFAC (L'Istituto di Fisica Applicata "Nello Carrara") Website, 2010, Available at: Hyperlink http://niremf.ifac.cnr.it/tissprop, Accessed February 1, 2012.
5. Klemm, M. and G. Troester, "EM energy absorption in the human body tissues due to UWB antennas," *Progress In Electromagnetics Research*, Vol. 62, 261–280, 2006.
6. Zhang, M. and A. Alden, "Calculation of whole-body sar from a 100 MHz dipole antenna," *Progress In Electromagnetics Research*, Vol. 119, 133–153, 2011.
7. Mohsin, S. A., "Concentration of the specific absorption rate around deep brain stimulation electrodes during MRI," *Progress In Electromagnetics Research*, Vol. 121, 469–484, 2011.
8. Otin, R. and H. Gromat, "Specific absorption rate computations with a nodal-based finite element formulation," *Progress In Electromagnetics Research*, Vol. 128, 399–418, 2012.
9. Theilmann, P. T., M. A. Tassoudji, E. H. Teague, D. F. Kimball, and P. M. Asbeck, "Computationally efficient model for UWB signal attenuation due to propagation in tissue for biomedical implants," *Progress In Electromagnetics Research B*, Vol. 38, 1–22, 2012.
10. Basar, M. R., M. F. B. A. Malek, K. M. Juni, M. I. M. Saleh, M. S. Idris, L. Mohamed, N. Saudin, N. A. Mohd Affendi, and A. Ali, "The use of a human body model to determine the variation of path losses in the human body channel in wireless capsule endoscopy," *Progress In Electromagnetics Research*, Vol. 133, 495–513, 2013.
11. Gabriel, C., "Compilation of the dielectric properties of body tissues at RF and microwave frequencies," Final Report Prepared for AFOSR/NL, 1996.
12. Walker, D. C., B. H. Brown, R. H. Smallwood, D. R. Hose, and D. M. Jones, "Modelled current distribution in cervical squamous tissue," *Physiol. Meas.*, Vol. 23, 159–168, 2002.

13. Huclova, S., D. Erni, and J. Fröhlich, "Modelling and validation of dielectric properties of human skin in the MHz region focusing on skin layer morphology and material composition," *J. Physics D: Applied Physics*, Vol. 45, 025301, 2012.
14. Singh, R. S., P. Tewari, J. L. Bourges, J. P. Hubschman, D. B. Bennett, Z. D. Taylor, H. Lee, E. R. Brown, W. S. Grundfest, and M. O. Culjat, "Terahertz sensing of corneal hydration," *Proc. 32nd Annumal Int'l Conf., IEEE EMBS*, 2010.
15. Spathmann, O., T. Fiedler, V. Hansen, M. Saviz, J. Streckert, M. Zang, M. Clemens, K. Statnikov, and U. Pfeiffer, "Attempts for exposure assessment in the THz frequency range using numerical computations," *Proc. EMC Europe*, Rome, Italy, 2012.
16. Gabriel, C., S. Gabriel, and E. Corthout, "The dielectric properties of biological tissues: I. Literature survey," *Phys. Med. Biol.*, Vol. 41, 2231–2249, 1996.
17. Gabriel, S., R. W. Lau, and C. Gabriel, "The dielectric properties of biological tissues: III. Parametric models for the dielectric spectrum of tissues," *Phys. Med. Biol.*, Vol. 41, 2271–2293, 1996.
18. Peyman, A., S. Holden, and C. Gabriel, "Measurement of the dielectric properties of biological tissues in vivo at microwave frequencies," Mobile Telecommunications and Health Research Programme, RUM 3, Final Report, 2005.
19. Gabriel, S., R. W. Lau, and C. Gabriel, "The dielectric properties of biological tissues: II. Measurements in the frequency range 10 Hz to 20 GHz," *Phys. Med. Biol.*, Vol. 41, 2251–2256, 1996.
20. Remington, L. A., *Clinical Anatomy of the Visual System,* 3rd Edition, Butterworth Heinemann, Ed., Elsevier, 2012.
21. Hayashi, S., T. Osawa, and K. Tohyama, "Comparative observations on corneas, with special reference to Bowman's layer and Descemet's membrane in mammals and amphibians," *J. Morphol.*, Vol. 254, No. 3, 247–258, 2002.
22. Kadler, K. E., D. F. Holmes, J. A. Trotter, and J. A. Chapman, "Collagen fibril formation," *Biochem. J.*, Vol. 316, 1–11, 1996.
23. Hahnel, C., S. Somodi, D. G. Weiss, and R. F. Guthoff, "The keratocyte network of human cornea: A three-dimensional study using confocal laser scanning fluorescence microscopy," *Cornea*, Vol. 19, No. 2, 185–193, 2000.
24. Almubrad, T. and S. Akhtar, "Structure of corneal layers, collagen fibrils, and proteoglycans of tree shrew cornea," *J. Molecular Vision*, Vol. 17, 2283–2291, 2011.
25. Boote, C., S. Hayes, M. Abahussin, and K. M. Meek, "Mapping

collagen organization in the human cornea: Left and right eyes are structurally distinct," *IOVS*, Vol. 47, 901–908, 2006.

26. Meek, K. M. and D. W. Leonard, "Ultrastructure of the corneal stroma: A comparative study," *Biophys. J.*, Vol. 64, 273–280, 1993.
27. Kim, J. H., K. Green, M. Martinez, and D. Paton, "Solute permeability of the corneal endothelium and Descemet's membrane," *Exp. Eye Res.*, Vol. 12, 231–238, 1971.
28. Sihvola, A., "Mixing rules with complex dielectric coefficients," *Subsurface Sensing Technologies and Applications*, Vol. 1, 393–415, 2000.
29. Gimsa, J., T. Müller, T. Schnelle, and G. Fuhr, "Dielectric spectroscopy of single human erythrocytes at physiological ionic strength: Dispersion of the cytoplasm," *Biochem. J.*, Vol. 71, 495–506, 1996.
30. Wei, Y. Z. and S. Sridhar, "Dielectric spectroscopy up to 20 GHz of $LiCl/H_2O$ solutions," *J. Chem. Phys.*, Vol. 92, 923–928, 1990.
31. Grant, H. E., "The dielectric method of investigating bound water in biological material: An appraisal of the technique," *Bioelectromagnetics*, Vol. 3, 17–24, 1982.
32. Pekonen, O., K. Kärkkäinen, A. Sihvola, and K. Nikoskinen, "Numerical testing of dielectric mixing rules by FDTD method," *Journal of Electromagnetic Waves and Applications*, Vol. 13, No. 1, 67–87, 1999.
33. Giordano, S., "Effective medium theory for dispersions of dielectric ellipsoids," *J. of Electrostatics*, Vol. 58, 59–76, 2003.
34. Peyman, A. and C. Gabriel, "Cole-Cole parameters for the dielectric properties of porcine tissues as a function of age at microwave frequencies," *Phys. Med. Biol.*, Vol. 55, N413–N419, 2010.
35. Dawkins, A. W. J., C. Gabriel, R. J. Sheppard, and E. H. Grant, "Electrical properties of lens material at microwave frequencies," *Phys. Med. Biol.*, Vol. 26, 1–9, 1981.
36. Pottel, R., D. Adolph, and U. Kaatze, "Dielectric relaxation in aqueous solutions of some dipolar organic molecules," *Berichte der Bunsengesellschaft für physikalische Chemie*, Vol. 79, 278–285, 1975.
37. Kaatze, U., "On the existence of bound water in biological systems as probed by dielectric spectroscopy," *Phys. Med. Biol.*, Vol. 35, 1663, 1990.
38. Jay, L., A. Brocas, K. Singh, J. C. Kieffer, I. Brunette, and

T. Ozaki, "Determination of porcine corneal layers with high spatial resolution by simultaneous second and third harmonic generation microscopy," *Optics Expres.*, Vol. 16, 16284–16293, 2008.

39. Michelacci, Y. M., "Collagens and proteoglycans of the corneal extracellular matrix," *Brazillian J. of Medical and Biological Research*, Vol. 36, 1037–1046, 2003.
40. Leonard, D. W. and K. M. Meek, "Refractive indices of the collagen fibrils and extrafibrillar material of the corneal stroma," *Biophys. J.*, Vol. 72, 1382–1387, 1997.
41. Ameen, D. B., M. F. Bishop, and T. McMullen, "A lattice model for computing the transmissivity of the cornea and sclera," *Biophys. J.*, Vol. 75, 2520–2531, 1998.
42. Hahnel, C., S. Somodi, C. Slowik, D. G. Weiss, and R. F. Guthoff, "Fluorescence microscopy and three-dimensional imaging of the porcine corneal keratocyte network," *Graefe's Arch. Clin. Exp. Ophthalmol.*, Vol. 235, 773–779, 1997.
43. Liebe, H. J., G. A. Hufford, and T. Manabe, "A model for the complex permittivity of water at frequencies below 1 THz," *Int'l J. Infrared and Millimeter Waves*, Vol. 12, 659–675, 1991.
44. Simeonova, M. and J. Gimsa, "The influence of the molecular structure of lipid membranes on the electric field distribution and energy absorption," *Bioelectromagnetics*, Vol. 27, 652–666, 2006.
45. Doughty, M. J. and W. Seabert, J. P. G. Bergmanson, and Y. Blocker, "A Descriptive and qualitative study of keratocytes of the corneal stroma of albino rabbits using transmission electron microscopy," *Tissues and Cells*, Vol. 33, 408–422, 2001.
46. Piersol, G. A., "Eye: Cornea," Vol. II, *Human Anatomy, Including Structure and Development and Practical Considerations*, 1913:1450, J. B. Lippincott Company, Philadelphia, 1919.